DMD Fast Forward. Published on September 7, 2010 as doi:10.1124/dmd.110.034330

The effect of immune-complex formation on the distribution of a novel antibody to the ovarian tumor antigen CA125

Cinthia V. Pastuskovas, William Mallet, Suzanna Clark, Margaret Kenrick, Mohammed Majidy, Michelle Schweiger, Marjie Van Hoy, Siao Ping Tsai, Gregory Bennett, Ben-Quan Shen, Sarajane Ross, Paul Fielder, Leslie Khawli, and Jay Tibbitts.

Pharmacokinetic and Pharmacodynamic Sciences (C.V. P., M. K., B. Q. S., P. F., L. K., J. T.), Cancer Targets (W. M.), Translational Oncology (S. C., S. R.), Pathology Labs (M. M., M. V. H.), Safety Assessment (M. S.), Assay and Automation Technology (S. P. T., G. B.). Genentech, Inc., South San Francisco, California.

DMD Fast Forward. Published on September 7, 2010 as DOI: 10.1124/dmd.110.034330
This article has not been copyedited and formatted. The final version may differ from this version.

a) Running Title: Preclinical distribution of an anti-MUC16 antibody

b) Corresponding Author: Jay Tibbitts, 640 E. Grand Ave., South San Francisco, CA 94080. Phone: 650-467-3194; FAX: 650-742-5234. E-mail: tibbitts @gene.com

c) Number of text pages: 27

Number of tables: 0

Number of figures: 6

Number of references: 37

Number of words in the Abstract: 243

Number of words in the Introduction: 704

Number of words in the Discussion: 814

d) Abbreviations: ADC, antibody-drug conjugate; AUC, area under the concentration-time curve; ELISA, enzyme-linked immunosorbent assay; IC, immune-complex; luc, luciferase-expressing; PBS, phosphate-buffered saline; PIs, phosphor-imaging plates; QWBA, quantitative whole-body autoradiography; SEC-HPLC, size exclusion high-performance liquid chromatography; SCID, severe combined immunodeficiency; TCA, trichloroacetic acid; µCi: microcurie.

DMD Fast Forward. Published on September 7, 2010 as DOI: 10.1124/dmd.110.034330
This article has not been copyedited and formatted. The final version may differ from this version.

ABSTRACT

3A5 is a novel antibody that binds repeated epitopes within CA125, an ovarian tumor antigen that is shed into circulation. Binding to shed antigen may limit the effectiveness of therapeutic antibodies due to unproductive immune-complex (IC) formation and/or altered antibody distribution. To evaluate this possibility, we characterized the impact of shed CA125 on the *in vivo* distribution of 3A5. *In vitro*, 3A5 and CA125 were found to form ICs in a concentration dependent manner. This phenomenon was then evaluated *in vivo* using quantitative whole body autoradiography (QWBA) to assess the tissue distribution of [^{125}I] 3A5 in an orthotopic OVCAR-3 tumor mouse model at different stages of tumor burden. Low doses of 3A5 (75 µg/kg) and pathophysiological levels of shed CA125 led to the formation of ICs *in vivo* that were rapidly distributed to the liver. Under these conditions, increased clearance of 3A5 from normal tissues was observed in mice bearing CA125 expressing tumors. Importantly, despite IC formation, 3A5 uptake by tumors was sustained over time. At a therapeutically relevant dose of 3A5 (3.5 mg/kg), IC formation was undetectable and distribution to normal tissues followed that of blood. Conversely, increased levels of radioactivity were observed in the tumors. These data demonstrate that CA125 and 3A5 do form ICs *in vivo*, and that the liver is involved in their uptake. However, at therapeutic doses of 3A5 and clinically relevant CA125 levels, IC formation consumes only a minor fraction of 3A5, and tumor targeting appears unaffected.

DMD Fast Forward. Published on September 7, 2010 as DOI: 10.1124/dmd.110.034330
This article has not been copyedited and formatted. The final version may differ from this version.

INTRODUCTION

Ovarian cancer is the fifth most common cause of cancer death in women. Each year, approximately 20,000 American women are diagnosed with ovarian cancer and about 15,000 die from the disease (American Cancer Society, 2007). Current treatment options consist of surgery followed by chemotherapy, and occasionally radiation therapy, but prognosis remains poor due to the highly metastatic potential of this disease (Piver et al., 1991) and long-term risk of tumor relapse after surgery. To improve therapeutic outcome, monoclonal antibodies specific for ovarian tumor-antigens are being developed (Schultes et al., 1998; Noujaim et al., 2001; Ehlen et al., 2005).

One such ovarian-specific tumor antigen is MUC16, a member of the mucin family of receptors (O'Brien et al., 2001; Yin and Lloyd, 2001) which is over-expressed on the membrane of epithelial ovarian cancer cells. The extracellular domain of MUC16, called CA125, is shed from the tumor cell surface (Beck et al., 1998). For many years the presence of shed CA125 in the serum has proven useful as a marker for not only the presence of ovarian cancer, but also for response to therapy and disease recurrence (Bast et al., 1983; Bast et al., 1998; Verheijen et al., 1999; Berek et al., 2008). While the expression pattern of MUC16 has made this protein a potentially important target for antibody therapy (Harris, 2004; Nicodemus and Berek, 2005), there is concern that shed CA125 may induce immune complex (IC) formation with therapeutic antibodies and prevent their effectiveness.

Here, we describe a novel CA125-specific antibody, named 3A5, which recognizes not a single epitope, but rather a repeated epitope within this tumor antigen. 3A5 was previously found to bind more sites per cell than an antibody that binds to a single epitope (Chen et al., 2007). This property is hypothesized to enhance the therapeutic effectiveness of 3A5, and explains why 3A5

DMD Fast Forward. Published on September 7, 2010 as DOI: 10.1124/dmd.110.034330
This article has not been copyedited and formatted. The final version may differ from this version.

is currently a component of an antibody-drug conjugate (ADC) strategy (Trail et al., 2003; Polakis, 2005; Wu and Senter, 2005; Chen et al., 2007; Junutula et al., 2008). This strategy consists of combining the targeting power of 3A5 with the chemotherapeutic effect of a cytotoxic drug, demonstrating potent anti-tumor activity in the OVCAR-3 ovarian tumor model (Chen et al., 2007; Junutula et al., 2008). Due to the multi-valency of 3A5, IC formation may have a greater impact on tumor targeting and/or *in vivo* distribution of this antibody in comparison with antibodies binding with a lower stoichiometry. To address this potential problem, we performed studies to determine the conditions and kinetics by which IC formation between 3A5 and CA125 occurs *in vitro,* to explore the tissue distribution of pre-formed 3A5-CA125 IC, and to characterize the *in vivo* impact of circulating CA125 on 3A5 distribution to target tissues at early and late stages of the disease, using an orthotopic ovarian cancer animal tumor model.

In this model, immune-compromised mice were injected with OVCAR-3 cells, a human ovarian carcinoma cell line, directly into the peritoneal cavity. This model recapitulates ovarian cancer in human patients in aspects such as extra-pelvic extension, ascites fluid accumulation, and at later stages dissemination within the peritoneal organs. In addition, this mouse model also resembles the human disease in its heterogeneity in the levels of shed CA125 antigen in the serum and ascites (Chen et al., 2007). Thus, this tumor model is thought to be a suitable representation of ovarian cancer in humans, providing clinically relevant information of the antitumor activity of the potential therapeutic agent.

Unlike subcutaneous xenograft models, a major challenge with this model is the quantitative assessment of drug distribution and progression of the tumor due to its localization within the organs in the peritoneum. Hence, in this study, *in vivo* bioluminescence imaging of luciferase-expressing OVCAR-3 (OVCAR-3/luc) tumor cells was used to allow the *in vivo*

characterization of tumor burden and quantitative whole body autoradiography (QWBA) was used to assess drug distribution; overcoming difficulties associated with the traditional tissue dissection.

In these studies, we found that the interaction of 3A5 with CA125 with results in the formation of IC *in vitro*. IC was also formed *in vivo* in the OVCAR-3 tumor model, in which the liver was identified as the major organ responsible for its uptake and clearance. IC formation did not, however, affect tumor targeting.

DMD Fast Forward. Published on September 7, 2010 as DOI: 10.1124/dmd.110.034330
This article has not been copyedited and formatted. The final version may differ from this version.

MATERIALS AND METHODS

Reagents and Cell lines. The anti-MUC16 antibody (3A5) was previously described (Chen et al., 2007). The CA125 human ovarian cancer antigen (Lot No L1040309M) was purchased from USBiological (Swampscott, MA). Genentech engineered recombinant humanized IgG1 specific for glycoprotein D (anti-gD) was used as an isotype control for 3A5. ^{125}I was obtained as sodium iodide in 10^{-5} N sodium hydroxide from Perkin Elmer (Boston, MA). 75 µg of 3A5 was labeled with 1 mCi iodine-125 [^{125}I] using the Iodogen method (Pierce Chemical Co., Rockford, IL). The pooled [^{125}I] 3A5 was > 97% trichloroacetic acid (TCA) precipitable. The resulting specific activity was 9.50 µCi/µg. OVCAR-3/luc cells were previously described (Chen et al., 2007).

***In Vitro* Studies.** Different concentrations of purified CA125 human cancer antigen and the [^{125}I] radiolabeled 3A5 were incubated in phosphate-buffered saline (PBS) for various times at 37°C to characterize the kinetics of IC formation over time. The following variables were evaluated for effects on IC formation: a) CA125 concentration (ranging from 0-2000 Units (U)/mL), b) [^{125}I] 3A5 concentration (ranging from 0.005 to 1.0 µg/mL), and c) incubation time (ranging from 0-24 hours). Size exclusion-high performance liquid chromatography (SEC-HPLC) was used to characterize IC formation. The samples were resolved by a Bio-Sep 4000 column (Phenomenex; Torrance, CA) using PBS as the mobile phase. Quantitation was based on the peak area under the concentration-time curve (AUC), divided by the sum of all peak AUCs x 100.

***In Vivo* Studies.** In all studies, mice were weighed, tagged, and housed in cages equipped with a coated wire floor to prevent animal contact with feces and urine. To prevent [^{125}I] .30 mg/mL of sodium iodide 1 and 24 hours prior to dosing with the radiolabeled dosing

DMD Fast Forward. Published on September 7, 2010 as DOI: 10.1124/dmd.110.034330
This article has not been copyedited and formatted. The final version may differ from this version.

material. All dosing materials were prepared at Genentech, Inc. the night prior to use and dose volumes (100 µL) were adjusted with the vehicle, PBS. Mice were distributed into groups and dosed as described in the Results section. Euthanasia of all animals was performed by IV injection of pentobarbital through the tail vein at specified time points. All studies were conducted in accordance with the Guide for the Care and Use of Laboratory Animals (1996). Data are presented as mean + standard deviation. Statistical analysis was performed using a 2 tail T-test, $p \leq 0.05$ was considered significant.

Tissue distribution of pre-formed ICs. Thirty normal female CD1 mice (Charles River Labs, Hollister, CA), 6–8 weeks old, weighing between 17.6–20.9 g, were used to determine if *in vitro* pre-formed ICs affected the distribution and clearance of [^{125}I] 3A5 in a normal mouse model. Pre-formed [^{125}I] 3A5-CA125 IC was prepared *in vitro* by incubating purified CA125 (2500 U/mL) with [^{125}I] 3A5 (1 µg/mL) for one hour at 37°C. Each mouse was given a single IV bolus injection of [^{125}I] 3A5-CA125 IC or [^{125}I] 3A5 alone (control group). The dose of radioactivity in both groups was 800 µCi/kg. At terminal time points (0.25, 1, 6, 24 and 120 hours, n=3/time point) blood (200 µL) was collected via cardiac puncture under general anesthesia into Lithium Heparin microtainers (BD Biosciences, San Jose, CA) and kept at 4°C. Plasma was separated from whole blood by centrifugation. Tissue distribution in this model was assessed by tissue dissection of major organs of distribution. The tissues harvested from each mouse were heart, kidneys, liver, lungs, spleen, duodenum, and large intestines (intestinal contents were rinsed out with ice cold PBS). All organs were rinsed with PBS and blotted dry, weighed and frozen at -70°C until total radioactivity counting. Counts per minute (CPM) in dissected tissues, plasma, and dosing solution were determined using a gamma-counter (Wallac 1470, PerkinElmer Life and Analytical Sciences). The CPM was then used to calculate the

DMD Fast Forward. Published on September 7, 2010 as DOI: 10.1124/dmd.110.034330
This article has not been copyedited and formatted. The final version may differ from this version.

percent of injected dose normalized to a gram of tissue (%ID/g) or milliliter of fluid (%ID/mL) by dividing injected CPM with CPM/g tissue x 100. Plasma TCA precipitation was used to measure antibody-bound radioactivity in circulation. Briefly, the precipitated radioactivity present in 20 µL of plasma was prepared by adding 200 µL of ice-cold 1% bovine serum albumin in PBS (pH 7.2) to each plasma sample and vortex mixing, followed by the addition of 500 µL of ice-cold 20% TCA and vortex mixing again. After 30 minutes of incubation on wet ice, the samples were centrifuged at 14,000 rpm for 5 minutes. The supernatant was aspirated, and the radioactivity in the pellet of each sample was quantified for 1 minute using the gamma counter. The radioactivity before and after TCA precipitation (x 100) was used to determine the percentage of antibody-bound radioactivity for each plasma sample.

Impact of circulating CA125 on 3A5 tissue distribution. Fifty C.B-17 ICR SCID female mice (Charles River Laboratories), weighing between 20-25 g were utilized to assess *in vivo* IC formation and distribution of 3A5 in mice bearing tumors that shed CA125 antigen into circulation. Mice were inoculated intraperitoneally (IP) with OVCAR-3/luc tumor cells and tumor burden was determined by bioluminescence as described in (Chen et al., 2007). Inoculated mice were observed at ventral view by bioluminescence on the day of cell inoculation to determine cell distribution and then once weekly thereafter. Mice with similar bioluminescence signals 2 weeks after cell inoculation were separated into two groups: a) early stage of tumor burden, at approximately 35 days post-inoculation, characterized as little ascites development and tumors within the peritoneal organs and b) late stage tumor burden, at approximately 75 days post-inoculation, characterized as established ascites and solid tumors within the peritoneal organs. Animals were weighed throughout the experiment and monitored closely for signs of

DMD Fast Forward. Published on September 7, 2010 as DOI: 10.1124/dmd.110.034330
This article has not been copyedited and formatted. The final version may differ from this version.

distress (including distended abdomen, pale skin, and lethargy). If signs of distress or a loss of >20% of original body weight were observed, the mice were euthanized.

The serum CA125 levels from tumor-bearing mice were measured prior to 3A5 dosing using a CA125 ELISA kit (Alpha Diagnostic International, San Antonio, TX) according to the protocol supplied by the manufacturer.

Mice at an early stage of tumor burden were given a single IV bolus injection via tail vein of 75 µg/kg of [^{125}I] 3A5, equivalent to 600 µCi/kg of radioactivity. Mice at a late stage of tumor burden study were given a single IV bolus injection of 75 µg/kg of either [^{125}I] 3A5 or [^{125}I] anti-gD (isotype control antibody) in addition to unlabeled antibody to complete a total dose of 3.5 mg/kg. Terminal time points were: 0.25, 8, 24, and 48 hours post-dose (n = 3/time point for tumor bearing mice and n=2/time point for non-tumor-bearing mice) for the early stage tumor burden study and 0.25, 8, 24, 48, and 120 hours post-dose for the late stage tumor burden study when using 3A5, and 0.25, 24, and 120 hours post-dose for the control isotype antibody (n = 3/time point). Blood was collected at terminal time points via retro-orbital bleed under isoflurane anesthesia (150 µL into Lithium Heparin microtainers) for plasma separation. Plasma was kept at -70°C until analysis by SEC-HPLC and TCA precipitation as described previously. Following euthanasia, animals were secured on a foam board and immersed in an alcohol bath at -70°C until the bodies were completely frozen. Tissue distribution of [^{125}I] 3A5 in the OVCAR-3/luc tumor bearing mice was assessed by quantitative whole body autoradiography (QWBA) using the whole-body cryosectioning technique developed by Ullberg and Larsson (Ullberg and Larsson, 1981). QWBA allowed for the tissue distribution assessment of the test antibodies avoiding the challenge of tissue dissection where tumors grow within the normal organs. Animals were embedded in 4% carboxymethylcellulose and stored at -70°C until sectioning.

DMD Fast Forward. Published on September 7, 2010 as DOI: 10.1124/dmd.110.034330
This article has not been copyedited and formatted. The final version may differ from this version.

Sagittal sections of 20 μm thickness were obtained using a cryostat microtome (Leica CM3600, Germany) at -20°C. The sections were collected at three levels of interest in the sagittal plane, and all major tissues, organs, and fluids were included in these levels. Sections were lyophilized and mounted on clear tape (Filmolux 610 soft PVC glossy sheets, 6" x 8", Neschen). The whole-body cryosections were covered with Mylar film (Fralock, Canoga Park, CA) and exposed overnight at room temperature to phosphor-imaging plates (PIs) (YBIP 2025MS, Fuji Film Medical Systems, Inc., Stamford, CT) along with [^{125}I] calibration standards. These were prepared from normal whole blood spiked with known concentrations of [^{125}I] ranging from 0.01 μCi/mL to 15 μCi/mL. After the exposure time, the PIs were scanned using a Fuji Film BAS-5000 scanner (Fuji Film Medical Systems, Inc.) to obtain digital images of the radioactivity in each section. The MicroComputer Imaging Device (MCiD Analysis™, Version 7, Imaging Research Inc., ON, Canada) was used to quantify the concentrations of radioactivity in the calibration standards and tissues of whole-body sections, as described by Potchoiba et al. (Potchoiba et al., 1995) for [^{14}C] xenobiotics. The quantitation method described here was demonstrated to be as accurate and precise as the values obtained from gamma or liquid scintillation counter methods (Potchoiba et al., 1995; Potchoiba et al., 1998; Busch et al., 2000; Steinke et al., 2000). The lower limit of quantification was determined by the lower detected concentration in the calibration standards (0.01 μCi/mL). The concentration of radioactivity from tissues was extrapolated from each standard curve as μCi/g of tissue, assuming that 1 g of tissue weight was equivalent to 1 mL, and converted to a percent of the injected dose. The [^{125}I] associated antibodies distributed equally to ascites and solid tumors; therefore both compartments were added together during the quantitation and are reported as ascites-tumor values.

DMD Fast Forward. Published on September 7, 2010 as DOI: 10.1124/dmd.110.034330
This article has not been copyedited and formatted. The final version may differ from this version.

RESULTS

IC formation *in vitro*. To determine the *in vitro* conditions under which CA125 and [^{125}I] 3A5 formed ICs, various concentrations of 3A5 were incubated with clinically relevant concentrations of CA125 (Bast et al., 1983). Thus, as represented in Figure 1A, CA125 at a fixed concentration of 1000 U/mL was incubated for 24 hours at 37°C, according to Haisma et al (Haisma et al., 1987), with increasing concentrations of [^{125}I] 3A5 (0.1, 0.5, and 1 µg/mL). After incubation, samples were analyzed by SEC-HPLC to determine the extent of IC formation. At a fixed CA125 concentration of 1000 U/mL, the addition of 0.1 ug/mL of [^{125}I] 3A5 resulted in approximately 40% of the antibody forming IC (Fig. 1A). As the antibody concentration was increased relative to CA125, the proportion of IC formation relative to the total antibody decreased (Fig. 1A). Similarly, when the [^{125}I] 3A5 concentration was fixed at 0.1 µg/mL in the presence of varying concentrations of CA125, IC formation was concentration dependent such that the percent of free 3A5 decreased with increasing CA125 antigen (Fig. 1B). In these studies, a CA125 concentration of 1000 U/mL with 0.1 µg/mL of 3A5 resulted in 40- 60% of the antibody formed ICs by 24 hours (Figs. 1A, 1B). Therefore, this concentration of CA125 and 3A5 was used to determine the kinetics of IC formation *in vitro* over 0, 0.5, 4, and 24 hours. The formation of ICs was rapid, with 80% of the total IC formation occurring within the first 0.5 hours (Fig. 1C). These data indicate that the proportion of IC formed between 3A5 and CA125 is dependent on the relative concentrations of the antigen and antibody. IC formation is enhanced when the concentration of CA125 is greater than that of 3A5.

Tissue distribution and clearance of ICs in normal mice. To determine if IC formation altered the kinetics of tissue distribution and clearance of [^{125}I] 3A5 in a normal mouse model, [^{125}I] 3A5-CA125 IC was pre-formed *in vitro* prior to administration in mice. In an effort to

DMD Fast Forward. Published on September 7, 2010 as DOI: 10.1124/dmd.110.034330
This article has not been copyedited and formatted. The final version may differ from this version.

more closely mimic the level of IC formation that may be observed in the clinic, ICs were generated by incubating 2500 U/mL of purified CA125 with 1 μg/mL of [^{125}I] 3A5, that resulted in a dose of 5,560 U/kg and 2 μg/kg of CA125 and [^{125}I] 3A5, respectively. SEC-HPLC confirmed that 10% of the 3A5 was present as IC (Fig 2A, left panel), as predicted from in vitro data (Fig. 1B). No IC was present in the control group dosing material (Fig 2A, right panel).

At 0.25 hours following dosing with [^{125}I] 3A5-CA125 IC or [^{125}I] 3A5 the SEC-HPLC profile of plasma showed no detectable IC peak whereas [^{125}I] 3A5 was present in plasma of mice dosed with [^{125}I] 3A5 (Fig 2B, left and right panels, respectively), suggesting that circulating 3A5-CA125 IC is cleared more rapidly than uncomplex 3A5.

The impact of IC formation on the tissue distribution of 3A5 was determined using tissue dissection for quantitation of total radioactivity. There was no substantial difference in the tissue distribution of [^{125}I] 3A5-CA125 IC or [^{125}I] 3A5, with exception of the liver (Fig 2C, left and right panels, respectively). Uptake of radioactivity at 0.25 hours post-dose was significantly higher (*$p<0.05$) in the livers from mice dosed with pre-formed IC when compared with that of mice dosed with [^{125}I] 3A5 alone. These data suggest a role for the liver in the rapid uptake of IC.

Overall, in both groups the highest %ID/g was observed in the blood and highly perfused organs (spleen>lungs>liver>kidney>heart), indicating equilibration between the blood and other normal tissues, resulting in a parallel decrease with blood concentrations (Fig. 2C).

Impact of circulating CA125 on 3A5 tissue distribution.

Early stage of ascites and tumor development. To explore whether tumors that shed CA125 would result in IC formation and alteration of the tissue distribution of 3A5, OVCAR-3/luc tumor cells were inoculated into mice (Chen et al., 2007). A model at an early stage of

DMD Fast Forward. Published on September 7, 2010 as DOI: 10.1124/dmd.110.034330
This article has not been copyedited and formatted. The final version may differ from this version.

ascites development and tumor burden, characterized by bioluminescence, was used investigate the interaction of the antibody with the circulating shed antigen with minimal interference of tumor burden. Circulating levels of CA125 ranged from 61 to 102 U/mL, as determined by ELISA. Based on the conditions that resulted in IC formation *in vitro*, it was predicted that circulating CA125 levels needed to be greater relative to the 3A5 concentrations to facilitate IC formation.. Therefore, a dose of [^{125}I] 3A5 (75µg/kg) to mice with an early stage of tumor burden was expected to result in approximately 10% IC formation.

In parallel, 75 µg/kg of [^{125}I] 3A5 was administered to non-tumor-bearing mice (without CA125).

In tumor-bearing mice, 8% of 3A5-related radioactivity was present as IC in plasma at 0.25 hours post-dose (Fig. 3A). At 8 hours post-dose, the products of IC degradation were detected in plasma, as evidenced by the presence of a lower molecular weight peak in SEC-HPLC. By 24 and 48 hours post-dose, plasma radioactivity was diminished to below the levels of detection. In contrast, plasma from non-tumor-bearing mice showed no evidence of IC formation at any time point and radioactivity clearance was slower than that of tumor-bearing mice (Fig. 3B).

To further characterize the *in vivo* catabolism of [^{125}I] 3A5 in plasma over the time course of the study, TCA precipitation was performed on plasma samples from tumor-bearing and non-tumor-bearing mice collected at terminal time points. In both groups, [^{125}I] 3A5 was approximately 100% precipitable at all time points (Fig. 3C and D), with the exception of the 8 hour post-dose samples from tumor-bearing mice where the percentage of precipitable radioactivity declined to 75%. These data are consistent with the degradation products observed by SEC-HPLC at 8 hours post-dose in these mice (Fig. 3A).

DMD Fast Forward. Published on September 7, 2010 as DOI: 10.1124/dmd.110.034330
This article has not been copyedited and formatted. The final version may differ from this version.

To assess the tissue distribution of [^{125}I] 3A5 in tumor-bearing and non-tumor-bearing mice, QWBA was utilized. Autoradiograms from tumor and non-tumor-bearing mice are shown in Fig. 4A and C, respectively; data are represented as %ID/g in Fig. 4B and D, respectively. Importantly, at 0.25 hours post-dose, radioactivity in the liver of tumor-bearing mice was two-fold higher than that in non-tumor-bearing mice (31.6 + 1.57%ID/g vs. 15.21 + 2.74%ID/g, respectively). These data confirm the role of the liver in the uptake of ICs. At remaining time points levels of radioactivity in the liver decreased in parallel with those in the blood. These data together suggest that a fraction of the low dose of 3A5 forms IC by 0.25h and it is taken by the liver while the remaining free 3A5 rapidly declines from blood. Thus, even if more CA125 becomes available in circulation the rapid clearance of antibody in blood may impair the formation of new IC over time. Consistent with previous evidence of degradation products at 8 hours post-dose in tumor-bearing mice, high radioactivity levels were observed in the intestines and stomach. This is indicative of the route of elimination of [^{125}I] degradation products and of the known role of the stomach in the absorption of free [^{125}I], respectively (Regoeczi, 1987). Ascites-tumor uptake of [^{125}I] 3A5 increased until 8 hours post-dose, and remained unchanged over the 48 hour time course of the study (Fig. 4B, inset).

In non-tumor-bearing mice, radioactivity was largely distributed in the blood. After equilibration with highly perfused organs (spleen > lungs > liver > kidney = bone marrow > heart), levels in the blood and tissues remained relatively sustained over the 24 hours post-dose (Fig. 4C and D).

Late stage ascites and tumor development. The distribution of [^{125}I] 3A5 was characterized in normal vs. tumor tissues in a more clinically relevant model: mice presenting with circulating CA125 levels consistent with those observed in ovarian cancer patients (Bast et

DMD Fast Forward. Published on September 7, 2010 as DOI: 10.1124/dmd.110.034330
This article has not been copyedited and formatted. The final version may differ from this version.

al., 1983) and with "late-stage" tumors. At this stage of tumor burden (75 days post-inoculation) circulating CA125 levels in mice ranged from 69 to 318 U/mL. Higher levels of CA125 were not achievable without compromising the animal's health. In this study a therapeutically relevant dose of 3A5 ([^{125}I] 3A5 + unlabeled 3A5 to complete a total dose of 3.5 mg/kg), as determined by tumor efficacy studies of a 3A5 ADC (Chen et al., 2007), was administered to mice bearing OVCAR-3/luc tumors. Following the IV bolus administration neither IC formation nor degradation products were detected in plasma at any time point as determined by SEC-HPLC and TCA precipitation (Fig. 5A and inset, respectively). QWBA assessment of [^{125}I] 3A5 tissue distribution in tumor-bearing mice is depicted in Fig. 5B and C, with data represented as %ID/g in Fig. 5C. These experiments revealed high radioactivity levels in the blood and highly perfused organs. Radioactivity levels in these normal tissues decreased in parallel with blood radioactivity. In contrast, the %ID/g in ascites-tumor increased by 8 hours post-dose and remained relatively unchanged over the remaining time-course of the study (Fig. 5B and C).

To determine the specificity of 3A5 uptake by ascites-tumor, the distribution of 3A5 distribution was compared with that of an isotype control antibody in tumor-bearing mice. Mice bearing OVCAR-3/luc tumors at a late stage of the disease were dosed with [^{125}I] anti-gD (isotype control antibody) + unlabeled anti-gD for a total dose of 3.5 mg/kg. Tissue-to-blood ratios, a measure of tissue-specific uptake, were calculated from mice dosed with isotype control or 3A5 antibody (Fig. 6A and B, respectively). A ratio >1, indicative of the specific uptake of an antibody by a tissue, was only observed at 120 hours in the ascites-tumor (8.85±1.04) of mice dosed with 3A5 (Fig. 6B), while ascites-tumor from the control antibody revealed ratios <1 (Fig. 6A). All normal tissues from 3A5 and control antibody had ratios < 1 at all time points (Fig. 6).

DMD Fast Forward. Published on September 7, 2010 as DOI: 10.1124/dmd.110.034330
This article has not been copyedited and formatted. The final version may differ from this version.

DISCUSSION

In recent years, therapeutic antibodies have been used to specifically target tumor cells based on their surface expression of unique antigens. In some cases, the antigen is shed from the cell surface into the circulation where the antibody may form ICs with the circulating antigen, potentially impacting therapeutic efficacy by preventing it from reaching the tumor, and/or altering the antibody kinetics of distribution and clearance (Bruno et al., 2005). A number of ovarian cancer pre-clinical and clinical studies have addressed the potential risks of shed antigen (Hagan et al., 1985; Haisma et al., 1987; Pimm et al., 1989; Kobayashi et al., 1993; Pimm, 1995; Sakahara et al., 1996; Davies et al., 1997; McQuarrie et al., 1997; Prinssen, 1998; Maeda et al., 2004). In ovarian cancer patients, IC formation was detected upon delivery of an anti-CA125 antibody. However, the effect of circulating CA125 antigen did not appear to compromise pharmacokinetics of the antibody when it was used in excess of the circulating antigen (Sakahara et al., 1996; McQuarrie et al., 1997).

Here we studied 3A5, a novel antibody (Chen et al., 2007) which binds to a repeated epitope on CA125, and is currently a component of an antibody-drug conjugate strategy for the treatment of epithelial ovarian cancer (Chen et al., 2007). Due to the avidity of 3A5 to CA125, IC formation could impact the delivery of the antibody to the tumors and induce unwanted toxicities in normal tissues. To address this, we performed a series of studies to assess IC formation *in vitro* and *in vivo*, as well as to characterize the impact of 3A5-CA125 interaction on the kinetics of 3A5 distribution.

We demonstrated that the *in vitro* interaction between [^{125}I] 3A5 and CA125 can result in IC formation. The proportions of ICs are dependent on the relative concentrations of antibody and antigen. Increased concentrations of CA125 and a low concentration of 3A5 resulted in a

DMD Fast Forward. Published on September 7, 2010 as DOI: 10.1124/dmd.110.034330
This article has not been copyedited and formatted. The final version may differ from this version.

proportional increase in IC formation (Fig. 1). Importantly, when the concentration of 3A5 was increased while that of the antigen was held constant, the proportion of IC was low relative to the total 3A5. The *in vitro* kinetics of IC formation was rapid, in line with that reported by Haisma et al (Haisma et al., 1987). Consistently, IC formation between 3A5 and circulating CA125 was detected *in vivo* in tumor-bearing mice only at low concentrations of the antibody relative to the antigen, which was determined by ELISA. When mice presenting with clinically relevant CA125 levels (69-318 U/mL) (Bast et al., 1983), were given a therapeutic dose of 3A5 (3.5 mg/kg) (Chen et al., 2007) no IC was detected. Collectively, these data suggest that IC formation at therapeutic 3A5 concentrations appears to consume a small fraction of the total 3A5. Further, whether ICs were administered pre-formed to normal mice, or formed *in vivo* in tumor-bearing mice, they were rapidly cleared from circulation, with the liver demonstrating a major role in the uptake, and degradation. Consistent with liver catabolism, there was evidence of IC degradation products in the plasma, the contents of the intestines, and the stomach, an organ known to absorb free [^{125}I] (Regoeczi, 1987). Aside from the liver, we observed no overall difference in tissue kinetics in normal mice dosed with either 3A5-CA125 IC pre-formed *in vitro*, or 3A5 alone (Fig. 2C). However, when IC was formed *in vivo* by administering a low dose of 3A5 (75 µg/kg) to tumor bearing mice, faster clearance of the antibody was observed in normal tissues of these mice when compared to 3A5 dosed to normal mice (Figs. 4A and B). This effect was not as pronounced when tumor-bearing mice received a therapeutically relevant dose of 3A5 (3.5 mg/kg) (Fig. 5B and C).

An important finding in these studies was that 3A5 distribution to the tumor was achieved despite IC formation. At the therapeutic dose of 3A5, persistent uptake of antibody in ascites-tumors was observed, with no IC detected and no uptake or accumulation in normal tissues.

DMD Fast Forward. Published on September 7, 2010 as DOI: 10.1124/dmd.110.034330
This article has not been copyedited and formatted. The final version may differ from this version.

Specificity of 3A5 for ascites-tumors was demonstrated by the high tissue-to-blood ratios, while the isotype control antibody and normal tissue ratios revealed blood related distribution only (Fig.6). These data indicate that despite the binding of 3A5 to repeated epitopes expressed within CA125, IC formation did not affect tumor targeting.

The data herein describe the circumstances under which IC forms *in vitro* and *in vivo*. In conclusion, the interaction between 3A5 and CA125 resulted in the formation of ICs that were rapidly distributed from circulation to the liver. At a therapeutically relevant dose, however, the proportion of IC relative to total 3A5 appeared to be minor, with a consequent greater distribution of uncomplexed 3A5 to the tumor. As a point of consideration, it remains possible that as the concentration of 3A5 decreases *in vivo* due to normal clearance, conditions may arise that result in a proportional increase in IC formation, a phenomenon that should be monitored clinically.

DMD Fast Forward. Published on September 7, 2010 as DOI: 10.1124/dmd.110.034330
This article has not been copyedited and formatted. The final version may differ from this version.

ACKNOWLEDGEMENTS

We thank Mike Reich, Hartmut Koeppen, Joel Morales, Daniela Bumbaca, Susan Spencer, Doug Leipold, and Frank-Peter Theil for their support to this study, and all our Genentech colleagues for helpful discussion and comments.

DMD Fast Forward. Published on September 7, 2010 as DOI: 10.1124/dmd.110.034330
This article has not been copyedited and formatted. The final version may differ from this version.

References

American Cancer Society I (2007) Facts and Figures, Atlanta.

Bast RC, Jr., Klug TL, St John E, Jenison E, Niloff JM, Lazarus H, Berkowitz RS, Leavitt T, Griffiths CT, Parker L, Zurawski VR, Jr. and Knapp RC (1983) A radioimmunoassay using a monoclonal antibody to monitor the course of epithelial ovarian cancer. *N Engl J Med* **309:**883-887.

Bast RC, Jr., Xu FJ, Yu YH, Barnhill S, Zhang Z and Mills GB (1998) CA 125: the past and the future. *Int J Biol Markers* **13:**179-187.

Beck EP, Moldenhauer A, Merkle E, Kiesewetter F, Jager W, Wildt L and Lang N (1998) CA 125 production and release by ovarian cancer cells in vitro. *Int J Biol Markers* **13:**200-206.

Berek JS, Taylor PT and Nicodemus CF (2008) CA125 velocity at relapse is a highly significant predictor of survival post relapse: results of a 5-year follow-up survey to a randomized placebo-controlled study of maintenance oregovomab immunotherapy in advanced ovarian cancer. *J Immunother* **31:**207-214.

Bruno R, Washington CB, Lu JF, Lieberman G, Banken L and Klein P (2005) Population pharmacokinetics of trastuzumab in patients with HER2+ metastatic breast cancer. *Cancer Chemother Pharmacol* **56:**361-369.

Busch U, Heinzel G and Nehmiz G (2000) Precision of measurement of tissue concentrations by RLG. *Regul Toxicol Pharmacol* **31:**S45-50.

Chen Y, Clark S, Wong T, Chen Y, Chen Y, Dennis MS, Luis E, Zhong F, Bheddah S, Koeppen H, Gogineni A, Ross S, Polakis P and Mallet W (2007) Armed antibodies targeting the mucin repeats of the ovarian cancer antigen, MUC16, are highly efficacious in animal tumor models. *Cancer Res* **67:**4924-4932.

Davies Q, Perkins AC, Frier M, Watson S, Lalani E and Symonds EM (1997) The effect of circulating antigen on the biodistribution of the engineered human antibody hCTM01 in a nude mice model. *Eur J Nucl Med* **24:**206-209.

Ehlen TG, Hoskins PJ, Miller D, Whiteside TL, Nicodemus CF, Schultes BC and Swenerton KD (2005) A pilot phase 2 study of oregovomab murine monoclonal antibody to CA125 as an immunotherapeutic agent for recurrent ovarian cancer. *Int J Gynecol Cancer* **15:**1023-1034.

Hagan PL, Halpern SE, Chen A, Krishnan L, Frincke J, Bartholomew RM, David GS and Carlo D (1985) In vivo kinetics of radiolabeled monoclonal anti-CEA antibodies in animal models. *J Nucl Med* **26:**1418-1423.

Haisma HJ, Battaile A, Stradtman EW, Knapp RC and Zurawski VR, Jr. (1987) Antibody-antigen complex formation following injection of OC125 monoclonal antibody in patients with ovarian cancer. *Int J Cancer* **40:**758-762.

Harris M (2004) Monoclonal antibodies as therapeutic agents for cancer. *Lancet Oncol* **5:**292-302.

Institute of Laboratory Animal Resources "Guide for the Care and Use of Laboratory Animals" (1996). *National Academy Press*.

Junutula JR, Raab H, Clark S, Bhakta S, Leipold DD, Weir S, Chen Y, Simpson M, Tsai SP, Dennis MS, Lu Y, Meng YG, Ng C, Yang J, Lee CC, Duenas E, Gorrell J, Katta V, Kim A, McDorman K, Flagella K, Venook R, Ross S, Spencer SD, Lee Wong W, Lowman HB, Vandlen R, Sliwkowski MX, Scheller RH, Polakis P and Mallet W (2008) Site-specific conjugation of a cytotoxic drug to an antibody improves the therapeutic index. *Nat Biotechnol* **26:**925-932.

Kobayashi H, Sakahara H, Saga T, Hosono M, Shirato M, Kanda H, Ishibashi K, Watanabe T, Endo K, Ishiwata I and et al. (1993) A human/mouse chimeric monoclonal antibody against CA125 for radioimmunoimaging of ovarian cancer. *Cancer Immunol Immunother* **37:**143-149.

Maeda T, Inoue M, Koshiba S, Yabuki T, Aoki M, Nunokawa E, Seki E, Matsuda T, Motoda Y, Kobayashi A, Hiroyasu F, Shirouzu M, Terada T, Hayami N, Ishizuka Y, Shinya N, Tatsuguchi A, Yoshida M, Hirota H, Matsuo Y, Tani K, Arakawa T, Carninci P, Kawai J, Hayashizaki Y, Kigawa T and Yokoyama S (2004) Solution structure of the SEA domain from the murine homologue of ovarian cancer antigen CA125 (MUC16). *J Biol Chem* **279:**13174-13182.

McQuarrie SA, Baum RP, Niesen A, Madiyalakan R, Korz W, Sykes TR, Sykes CJ, Hor G, McEwan AJ and Noujaim AA (1997) Pharmacokinetics and radiation dosimetry of 99Tcm-labelled monoclonal antibody B43.13 in ovarian cancer patients. *Nucl Med Commun* **18:**878-886.

Nicodemus CF and Berek JS (2005) Monoclonal antibody therapy of ovarian cancer. *Expert Rev Anticancer Ther* **5:**87-96.

Noujaim AA, Schultes BC, Baum RP and Madiyalakan R (2001) Induction of CA125-specific B and T cell responses in patients injected with MAb-B43.13--evidence for antibody-mediated antigen-processing and presentation of CA125 in vivo. *Cancer Biother Radiopharm* **16:**187-203.

O'Brien TJ, Beard JB, Underwood LJ, Dennis RA, Santin AD and York L (2001) The CA 125 gene: an extracellular superstructure dominated by repeat sequences. *Tumour Biol* **22:**348-366.

Pimm MV (1995) Circulating antigen: bad or good for immunoscintigraphy? *Nucl Med Biol* **22:**137-145.

Pimm MV, Durrant LG and Baldwin RW (1989) Influence of circulating antigen on the biodistribution and tumour localization of radiolabelled monoclonal antibody in a human tumour: nude mouse xenograft model. *Eur J Cancer Clin Oncol* **25:**1325-1332.

Piver MS, Baker TR, Piedmonte M and Sandecki AM (1991) Epidemiology and etiology of ovarian cancer. *Semin Oncol* **18:**177-185.

Polakis P (2005) Arming antibodies for cancer therapy. *Curr Opin Pharmacol* **5:**382-387.

Potchoiba MJ, Tensfeldt TG, Nocerini MR and Silber BM (1995) A novel quantitative method for determining the biodistribution of radiolabeled xenobiotics using whole-body cryosectioning and autoradioluminography. *J Pharmacol Exp Ther* **272:**953-962.

Potchoiba MJ, West M and Nocerini MR (1998) Quantitative comparison of autoradioluminographic and radiometric tissue distribution studies using carbon-14 labeled xenobiotics. *Drug Metab Dispos* **26:**272-277.

Prinssen (1998) Biodistribution of 111In-labelled engineered human antibody CTMO1 (hCTMO1) in ovarian cancer patients: influence of prior administration of unlabelled hCTMO1. *Cancer Immunol. Immunother. Sep 47(1)***:**39-46.

Regoeczi E (1987) Iodine Labeled Plasma Protein. *CRC Press* **Vol II Part B:**645-648.

Sakahara H, Hosono M, Kobayashi H, Yao Z, Saga T, Yano S, Endo K, Mori T and Konishi J (1996) Effect of circulating antigen on immunoscintigraphy of ovarian cancer patients using anti-CA125 monoclonal antibody. *Jpn J Cancer Res* **87:**655-661.

Schultes BC, Baum RP, Niesen A, Noujaim AA and Madiyalakan R (1998) Anti-idiotype induction therapy: anti-CA125 antibodies (Ab3) mediated tumor killing in patients treated with Ovarex mAb B43.13 (Ab1). *Cancer Immunol Immunother* **46:**201-212.

Steinke W, Archimbaud Y, Becka M, Binder R, Busch U, Dupont P and Maas J (2000) Quantitative distribution studies in animals: cross-validation of radioluminography versus liquid-scintillation measurement. *Regul Toxicol Pharmacol* **31:**S33-43.

Trail PA, King HD and Dubowchik GM (2003) Monoclonal antibody drug immunoconjugates for targeted treatment of cancer. *Cancer Immunol Immunother* **52:**328-337.

Ullberg S and Larsson B (1981) Whole-body autoradiography. *Methods Enzymol* **77:**64-80.

Verheijen RH, von Mensdorff-Pouilly S, van Kamp GJ and Kenemans P (1999) CA 125: fundamental and clinical aspects. *Semin Cancer Biol* **9:**117-124.

Wu AM and Senter PD (2005) Arming antibodies: prospects and challenges for immunoconjugates. *Nat Biotechnol* **23:**1137-1146.

Yin BW and Lloyd KO (2001) Molecular cloning of the CA125 ovarian cancer antigen: identification as a new mucin, MUC16. *J Biol Chem* **276:**27371-27375.

DMD Fast Forward. Published on September 7, 2010 as DOI: 10.1124/dmd.110.034330
This article has not been copyedited and formatted. The final version may differ from this version.

Footnotes

Financial support for this work was provided by Genentech, Inc.

Address correspondence to: Dr. Jay Tibbitts, Genentech, Inc. 640 E. Grand Ave. South San Francisco, CA 94080. E-mail: tibbitts @gene.com

DMD Fast Forward. Published on September 7, 2010 as DOI: 10.1124/dmd.110.034330
This article has not been copyedited and formatted. The final version may differ from this version.

Legends for figures

Figure 1. *In vitro* formation of 3A5 and CA125 immune complex. **(A)** Increasing concentrations of [^{125}I] 3A5 with a fixed purified CA125 concentration of 1000 U/mL. (**B)** Increasing concentrations of purified CA125 with a fixed [^{125}I] 3A5 concentration of 0.1 µg/mL. The y-axis represents the percent peak area. The x-axis represents the different concentrations of either antibody or antigen, respectively. **(C)** Percent of IC formation between 0.1 µg/mL [^{125}I] 3A5 + 1000 U/mL purified CA125 over 24 hours incubation time period at 37°C. Data are presented as percent IC formation (%IC) and percent of free 3A5 (%3A5) of two replicates per time point, per condition.

Figure 2. Pre-formed 3A5 ICs are rapidly cleared by the liver in mice. SEC-HPLC chromatograms of the dosing solution and plasma samples from normal mice at 0.25 hours post-dose with either the pre-formed IC; **(A, left panel)** or [^{125}I] 3A5 alone **(A, right panel)**. **(B, left panel)** Plasma profiles from normal mice after IV dose of the pre-formed IC showing IC clearance from circulation at 0.25 hours post-dose. **(B, right panel)** Plasma profile from normal mice dosed with the antibody alone at 0.25 hours post-dose showing a similar profile to that of the dosing solution. Overlapped profiles from three independent animals in each group at 0.25 hours sampling time are shown. **(C, left panel)** Graphs represent %ID/g in normal mice after single IV bolus injection of [^{125}I] 3A5+ CA125 or **(C, right panel)** [^{125}I] 3A5 alone. Tissue distribution was determined by the tissue dissection method at 0.25, 1, 6, 24, or 120 hours post-dose. Data are expressed as the mean + standard deviation values of three animals per time point in

DMD Fast Forward. Published on September 7, 2010 as DOI: 10.1124/dmd.110.034330
This article has not been copyedited and formatted. The final version may differ from this version.

each group. Statistically significant liver uptake (*) was observed in mice dosed with the pre-formed IC compared with liver from mice dosed with [^{125}I] 3A5 alone ($p \leq 0.05$).

Figure 3. 3A5 forms ICs in OVCAR-3/luc tumor-bearing mice. SEC-HPLC profiles of representative plasma samples collected at indicated time-points following single IV dose of 75 µg/kg of [^{125}I] 3A5 into **(A)** OVCAR-3/luc tumor-bearing mice with circulating levels of CA125 or **(B)** non-tumor-bearing mice. The TCA-precipitable fraction of [^{125}I] 3A5 in plasma following IV administration into **(C)** OVCAR-3/luc tumor-bearing mice with circulating levels of CA125 and **(D)** non-bearing-tumor mice. Data are expressed as the mean + standard deviation values of three animals per time point in each group, with the exception of non-tumor-bearing mice at 8 and 24 hours with n=2.

Figure 4. 3A5 distributes to ascites-tumor in OVCAR-3/luc tumor-bearing mice despite IC formation. Representative whole-body sagittal sections of a mouse at different time points following [^{125}I] 3A5 administration. Anterior and posterior sectioning levels depict ascites-tumor and major organs of distribution, respectively. Left panel shows digital pictures of the sections for anatomical localization purposes. Right panel shows the autoradiograms with the distribution of [^{125}I] 3A5 after an IV dose of 75 µg/kg into **(A)** OVCAR-3/luc tumor-bearing mice at an early stage of tumor burden, and **(C)** non-tumor-bearing mice. Tissue distribution was determined by QWBA at 0.25, 8, 24, and 48 hours post-dose. The standard curve is represented as a pseudo-color heat-map, inserted above the autoradiograms.. Graphs represent %ID/g after single IV injection of 75 µg/kg of [^{125}I] 3A5 into (**B)** OVCAR-3/luc tumor-bearing mice (inset displays 3A5 uptake by

DMD Fast Forward. Published on September 7, 2010 as DOI: 10.1124/dmd.110.034330
This article has not been copyedited and formatted. The final version may differ from this version.

tumor on a smaller scale) and (**D)** non-tumor-bearing mice. Data are expressed as the mean + standard deviation values of three animals per time point, with the exception of non-tumor-bearing mice at 8 and 24 hours where n=2. Significant differences (*) in the extent of [^{125}I] 3A5 distribution to the liver and blood were observed in the tumor versus non-tumor-bearing mice (* $p \leq 0.05$).

Figure 5. Immune complex is not detected at therapeutically relevant dose of 3A5. **(A)** Plasma SEC-HPLC profile from OVCAR-3/luc tumor-bearing mice with circulating levels of CA125 after a single IV dose of 3.5 mg/kg ([^{125}I] 3A5 + unlabelled 3A5). Inset displays the percent of antibody that was TCA-precipitable from plasma samples over time. Data is expressed as the mean + standard deviation of three animals per time point. **(B)** Representative whole-body sagittal sections of OVCAR-3/luc tumor-bearing mice at different time points post-dose. Anterior and posterior sectioning levels depict ascites-tumor and major organs of distribution, respectively. Left panel shows digital pictures of the sections for anatomical localization purposes. Right panel shows the autoradiograms with the distribution of 3.5 mg/kg ([^{125}I] 3A5+ unlabelled 3A5) at 0.25, 8, 24, 48, and 120 hours. The standard curve is represented as a pseudo-color heat-map, inserted above the autoradiograms. Tissue distribution was assessed by QWBA. **(C)** Graph represents %ID/g after single IV dose of 3.5 mg/kg ([^{125}I] 3A5+ unlabelled 3A5) into OVCAR-3/luc tumor-bearing mice at a late stage of tumor burden with measurable levels of CA125. Data are expressed as the mean + standard deviation values of three animals per time point.

DMD Fast Forward. Published on September 7, 2010 as DOI: 10.1124/dmd.110.034330
This article has not been copyedited and formatted. The final version may differ from this version.

Figure 6. Tumor- to-blood ratio of 3A5 or control antibody after a single IV dose of 3.5 mg/kg of ([^{125}I] 3A5+ unlabelled 3A5) or ([^{125}I] anti-gD + unlabelled anti-gD into OVCAR-3/luc tumor-bearing mice at a late stage of tumor burden at 0.25, 24, and 120 hours post-dose. Data are expressed as the mean + standard deviation values of three animals per time point.

Figure 1

A

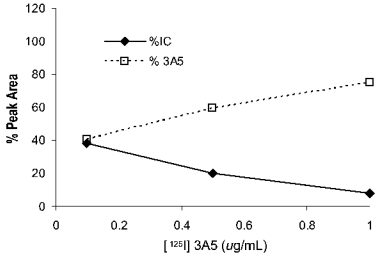
120
100
80
60
40
20
0
% Peak Area
%IC
% 3A5
0
0.2
0.4
0.6
0.8
1
[125I] 3A5 (ug/mL)

B

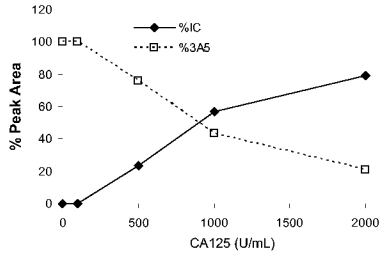
120
100
80
60
40
20
0
% Peak Area
%IC
%3A5
0
500
1000
1500
2000
CA125 (U/mL)

C

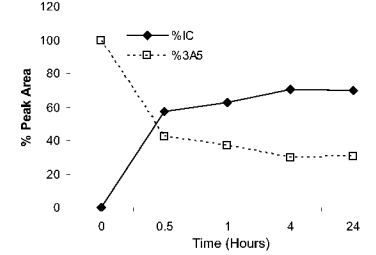
120
100
80
60
40
20
0
% Peak Area
%IC
%3A5
0
0.5
1
4
24
Time (Hours)

Figure 2

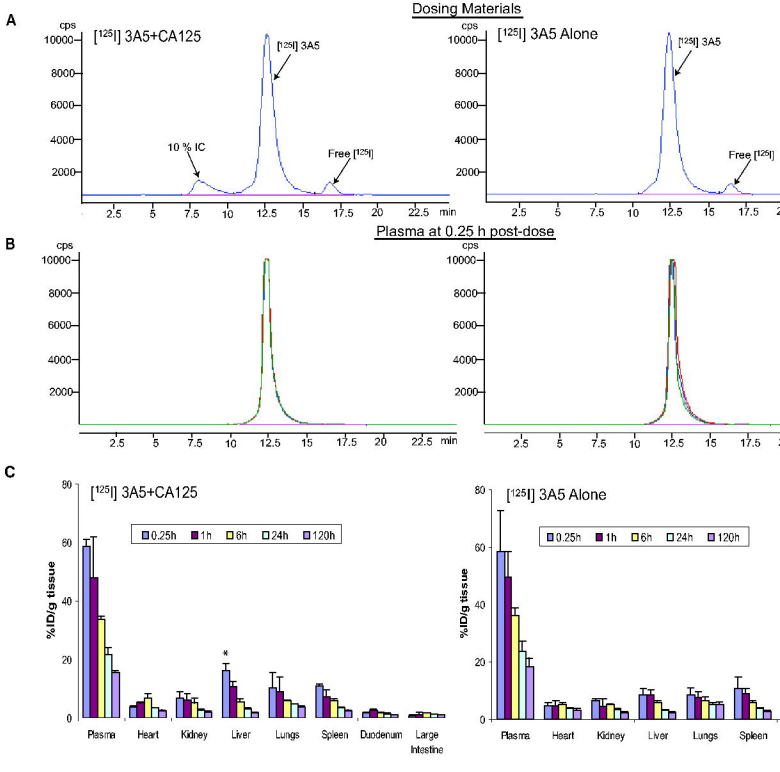
A
Dosing Materials
cps
[125I] 3A5+CA125
[125I] 3A5
10 % IC
Free [125I]
[125I] 3A5 Alone
[125I] 3A5
Free [125I]
min
B
Plasma at 0.25 h post-dose
cps
min
C
[125I] 3A5+CA125
0.25h
1h
6h
24h
120h
%ID/g tissue
Plasma
Heart
Kidney
Liver
Lungs
Spleen
Duodenum
Large Intestine
*
[125I] 3A5 Alone
0.25h
1h
6h
24h
120h
%ID/g tissue
Plasma
Heart
Kidney
Liver
Lungs
Spleen

Figure 3

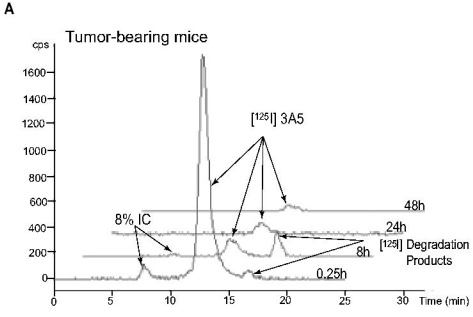
A
Tumor-bearing mice
cps
1600
1400
1200
1000
800
600
400
200
0
[125I] 3A5
48h
8% IC
24h
8h
[125I] Degradation Products
0.25h
0
5
10
15
20
25
30
Time (min)

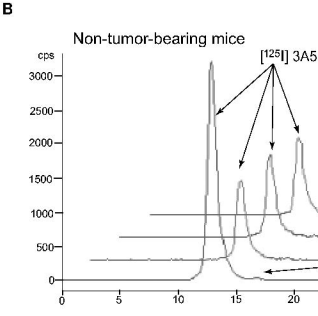
B
Non-tumor-bearing mice
cps
3000
2500
2000
1500
1000
500
0
[125I] 3A5
0
5
10
15
20

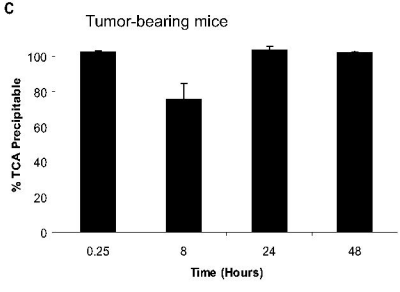
C
Tumor-bearing mice
% TCA Precipitable
100
80
60
40
20
0
0.25
8
24
48
Time (Hours)

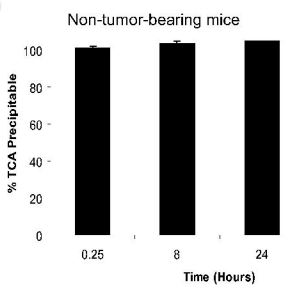
D
Non-tumor-bearing mice
% TCA Precipitable
100
80
60
40
20
0
0.25
8
24
Time (Hours)

Figure 4

A

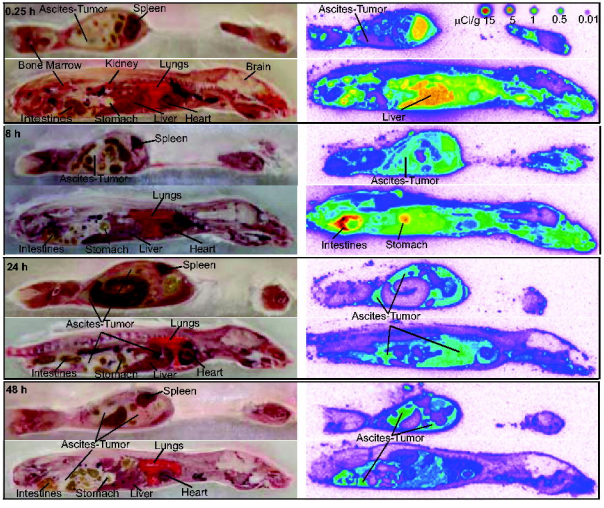
0.25 h
Ascites-Tumor
Spleen
Bone Marrow
Kidney
Lungs
Brain
Intestines
Stomach
Liver
Heart
µCi/g 15
5
1
0.5
0.01
8 h
24 h
48 h

B

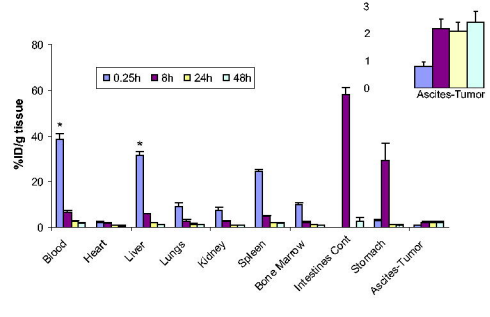
%ID/g tissue
0.25h
8h
24h
48h
Blood
Heart
Liver
Lungs
Kidney
Spleen
Bone Marrow
Intestines Cont
Stomach
Ascites-Tumor

Figure 4 (Continued)

C

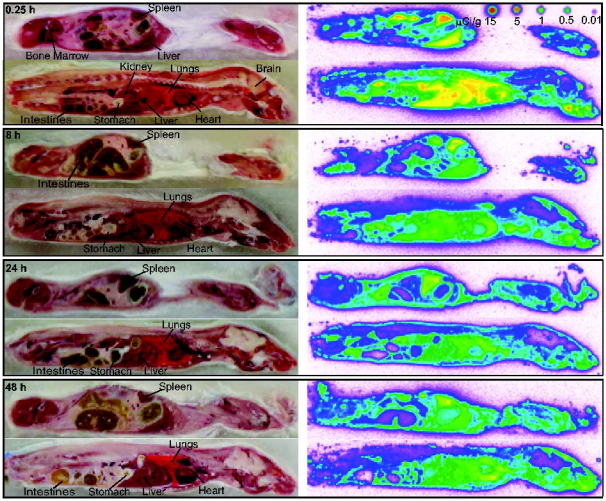

D

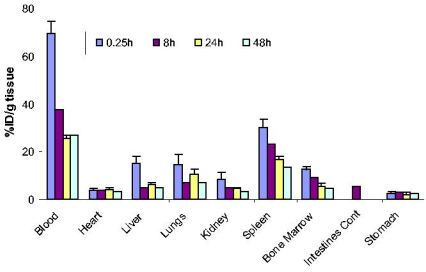

Figure 5

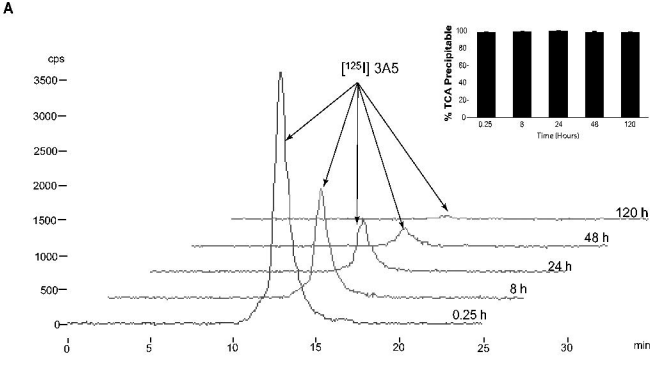
A
cps
3500
3000
2500
2000
1500
1000
500
0
[125I] 3A5
120 h
48 h
24 h
8 h
0.25 h
0
5
10
15
20
25
30
min
% TCA Precipitable
100
80
60
40
20
0
0.25
8
24
48
120
Time (Hours)

Figure 5 (Continued)

B

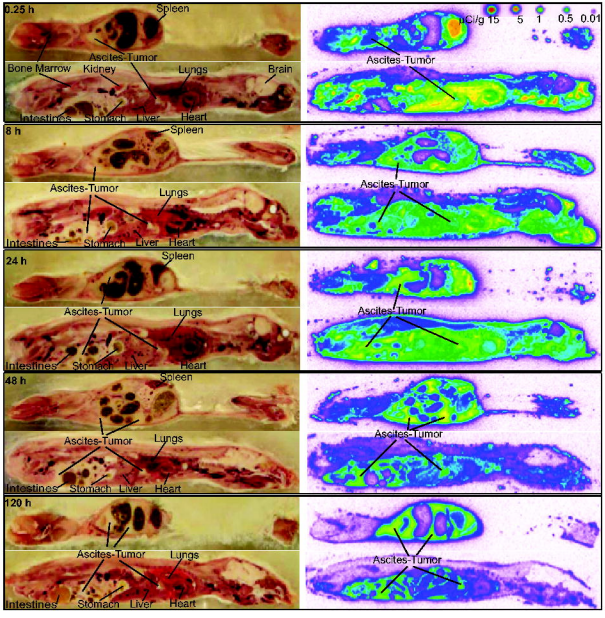

C

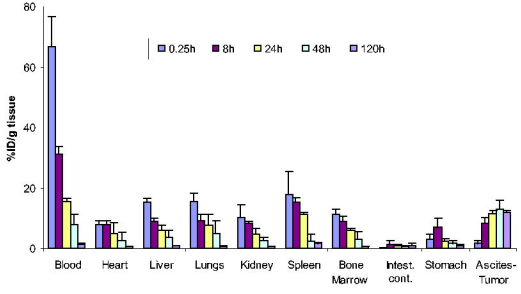

Figure 6

A

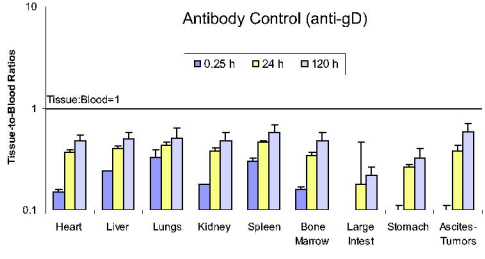
Antibody Control (anti-gD)
0.25 h
24 h
120 h
Tissue:Blood=1
Tissue-to-Blood Ratios
10
1
0.1
Heart
Liver
Lungs
Kidney
Spleen
Bone Marrow
Large Intest
Stomach
Ascites-Tumors

B

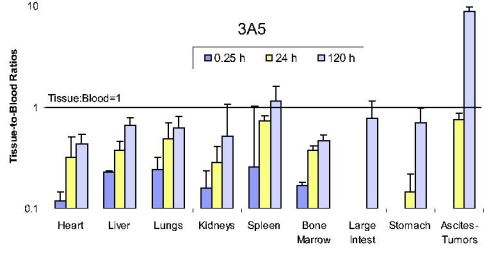
3A5
0.25 h
24 h
120 h
Tissue:Blood=1
Tissue-to-Blood Ratios
10
1
0.1
Heart
Liver
Lungs
Kidneys
Spleen
Bone Marrow
Large Intest
Stomach
Ascites-Tumors